Supplementary Information

Monomer Conversion Enables Chemical Recycling of High-Performance Plastics and Carbon Fiber Composites without Monomer Separation

Haoxiang Sun,[a] *Xiaohan Wang,* [a] *Xu Fang,* [a] *Xiang Li,* [a] *Wenjie Wang,*[a] *Xingyuan Lu**[a] *and Junqi Sun**[ab]

[a]State Key Laboratory of Supramolecular Structure and Materials, College of Chemistry, Jilin University, Changchun 130012, P. R. China

[b]Department of Chemistry, College of Science, Yanbian University, Yanji 133002, P. R. China

E-mail: xylu@jlu.edu.cn; sun_junqi@jlu.edu.cn

Experimental Section

Materials. Benzaldehyde, 4-formylbenzoic acid, and anhydrous magnesium sulfate ($MgSO_4$) were purchased from Innochem. Oxalyl chloride, triethylamine (TEA), and anhydrous potassium carbonate (K_2CO_3) were obtained from Tokyo Chemical Industry (TCI). 4,4′-(Hexafluoroisopropylidene)diphenol (HFPP), 4,4′-difluorobenzophenone (DFBP) and deuterated hexafluoroisopropanol (HFIP-d_2) were purchased from Aladdin. 4-Fluoro-3-(trifluoromethyl)aniline (FTMA) was obtained from Adamas. Plain-weave carbon fiber (CF) fabrics were supplied by Jilin Chemical Fiber Group Co., Ltd. Prior to use in the fabrication of CF-reinforced polymer composites (CFRCs), the CF fabrics were incinerated in air and subsequently soaked in methanol at 40 °C to remove the sizing agents. The treated CF fabrics were then washed with ethanol and dried thoroughly before use.

Characterizations. ^1H NMR spectra were recorded on a Bruker 500 MHz spectrometer. Fourier transform infrared (FT-IR) spectra were collected using a Bruker VERTEX 80 V FT-IR spectrometer. Tensile stress-strain curves were measured at room temperature using a universal testing machine (Instron 68TM-5) at a stretching speed of 50 mm min^{-1}. Thermogravimetric analysis (TGA) of the *r*PAEK plastics was performed on a TA Instruments Q500 thermogravimetric analyzer. Each sample (~6 mg) was heated from 30 to 800 °C at a rate of 10 °C min^{-1} under nitrogen. The glass transition temperatures (Tg) of the plastics were determined using differential scanning calorimetry (DSC, TA Instruments Q200). Each sample (~5 mg) was heated from 100 to 250 °C at a rate of 10 °C min^{-1} under a nitrogen flow. Scanning electron microscopy (SEM) images were obtained using an XL30 ESEM FEG scanning electron microscope. Raman spectra were recorded using a LabRAM ARAMIS Smart Raman spectrometer with an excitation wavelength of 633 nm. The intrinsic viscosities ([η]) of *r*PAEK, *r*PAEK$_{2.6k}$ and *r*PAEK$_{8.2k}$ were measured using an Ubbelohde viscometer in N-methyl-2-pyrrolidone (NMP) at 25 °C.

Calculation of the Molecular Weights of PAEK, PAEK$_{2.6k}$ and PAEK$_{8.2k}$. The number-average molecular weights (M_n) of PAEK, PAEK$_{2.6k}$, and PAEK$_{8.2k}$ were calculated based on the integral areas of peaks *a* and *i* in their ^{1}H NMR spectra according to the following equations:

$$n = \frac{number\ of\ repeating\ units}{number\ of\ polymer\ chains} = \frac{Area(i)/4}{Area(a)/4}$$

$$M_n = M_{repeating\ unit} * n + M_{end\ group} = (514.10n + 654.12)\ \mathrm{Da}$$

where A_i and A_a represent the integral areas of peaks *i* and *a*, respectively. The integral of peak *i* was divided by 4 because each repeating unit contains four hydrogen atoms. Similarly, the integral of peak *a* was divided by 4 because each polymer chain contains four hydrogen atoms from the two terminal amino groups.

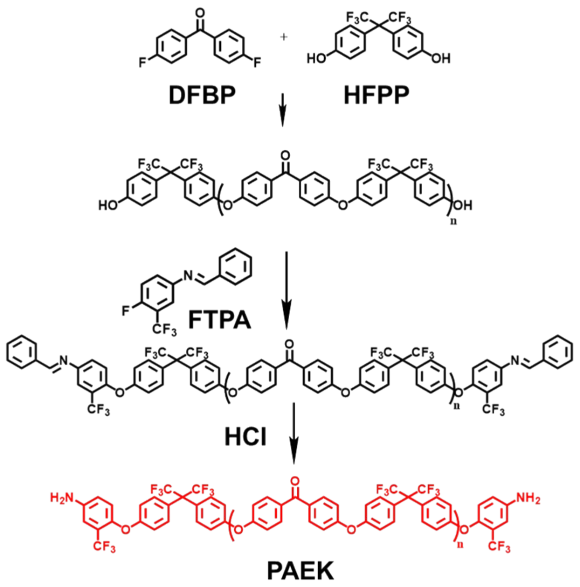

Fig. S1. Synthetic routes of PAEK.

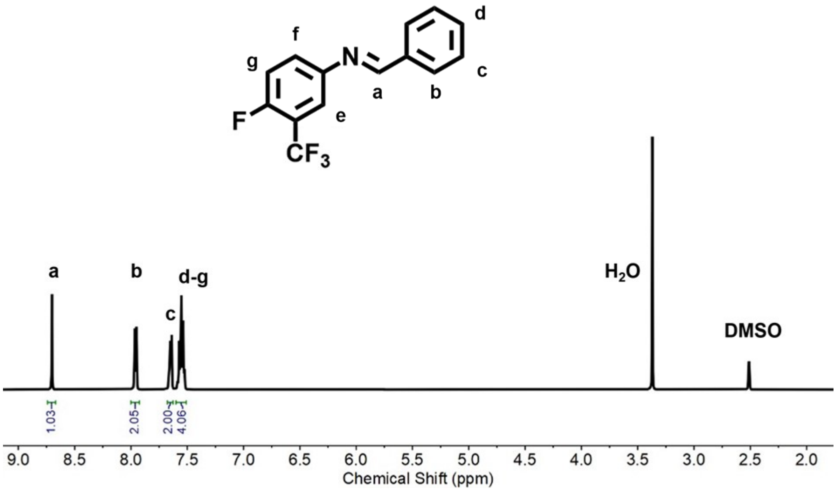

Fig. S2. ^{1}H NMR spectrum of FTPA.

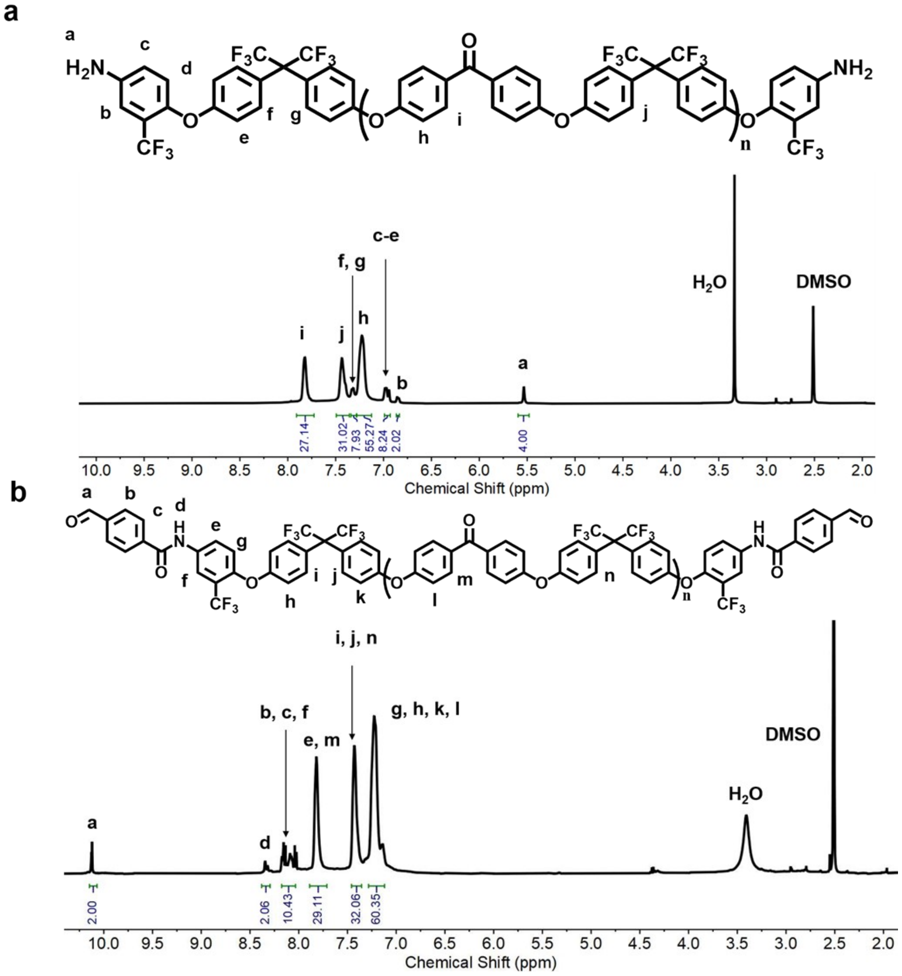

Fig. S3. ^{1}H NMR spectra of PAEK (a) and PA$_2$EK (b).

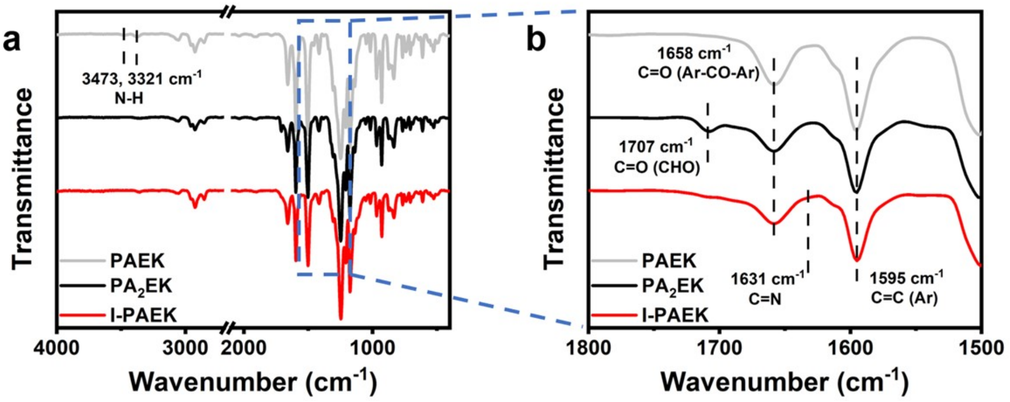

Fig. S4. FT-IR spectra of PAEK, PA$_2$EK, and I-PAEK.

In the FT-IR spectrum of PAEK, the peaks at 3473 and 3321 cm^{-1} correspond to the N-H stretching vibrations, while the peak at 1658 cm^{-1} is attributed to the C=O stretching vibration of the ketone groups. In the FT-IR spectrum of PA$_2$EK, the N-H stretching bands at 3473 and 3321 cm^{-1} disappear, and a new peak at 1707 cm^{-1} appears, corresponding to the C=O stretching vibration of the formyl groups, indicating the successful synthesis of PA$_2$EK. In the FT-IR spectrum of I-PAEK, the peak at 1707 cm^{-1} disappears, and a characteristic imine (C=N) stretching band appears at 1631 cm^{-1}, confirming the formation of the I-PAEK.

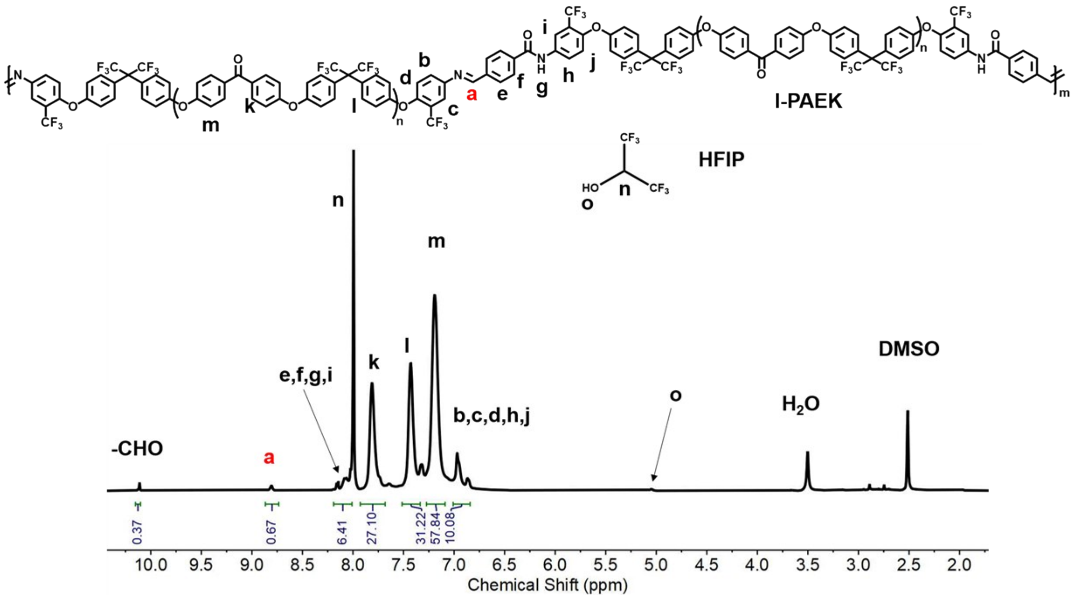

Fig. S5. ^{1}H NMR spectrum of I-PAEK measured in the mixture of DMSO-d$_6$ and HFIP-d$_2$ (v/v=5/1). A clear signal at 8.8 ppm is observed and assigned to the imine proton, confirming the formation of imine bonds in I-PAEK. During the NMR measurement, a small fraction of the imine bonds underwent cleavage because of the acidity of HFIP-d$_2$, as evidenced by the weak aldehyde proton signal at 10.2 ppm.

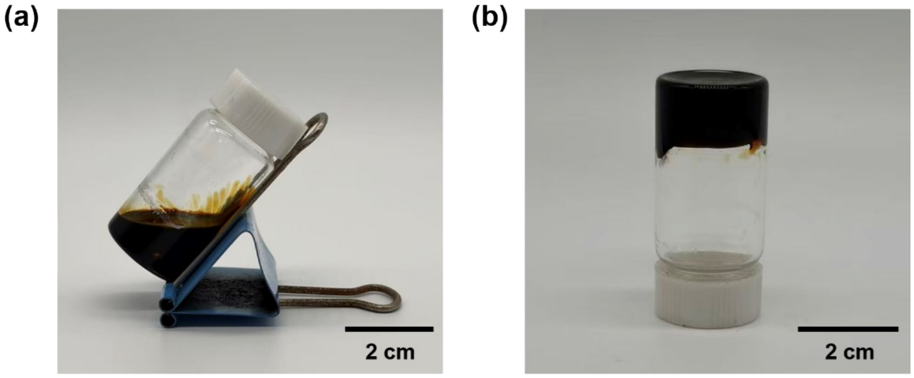

Fig. S6. Digital images of the hot NMP solution of I-PAEK (a) and the corresponding gel formed upon cooling to room temperature (b).

Table S1. Summary of mechanical properties of *r*PAEK, *r*PAEK$_{2.6k}$ and *r*PAEK$_{8.2k}$ plastics.

	Tensile Strength (MPa)	Young's Modulus (GPa)	Strain at Break (%)
*r*PAEK	85.8 ± 1.4	2.04 ± 0.13	6.8 ± 0.3
*r*PAEK$_{2.6k}$	65.0 ± 1.3	2.00 ± 0.15	4.0 ± 0.3
*r*PAEK$_{8.2k}$	56.3 ± 1.9	1.30 ± 0.08	5.6 ± 0.2

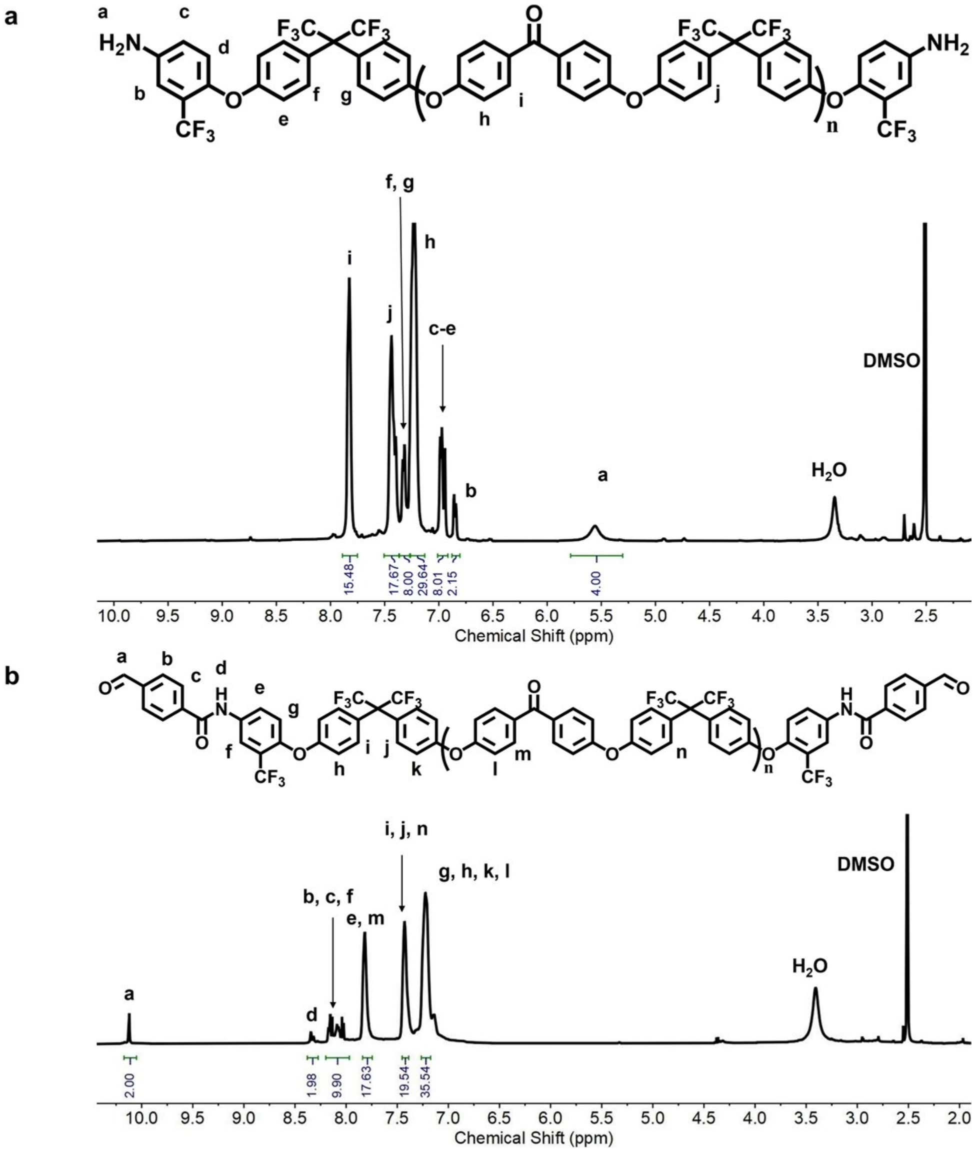

Fig. S7. ^{1}H NMR spectra of PAEK$_{2.6k}$ (a) and PA$_2$EK$_{2.6k}$ (b). According to the NMR data, the M_n of PAEK$_{2.6k}$ is ~2643.69.

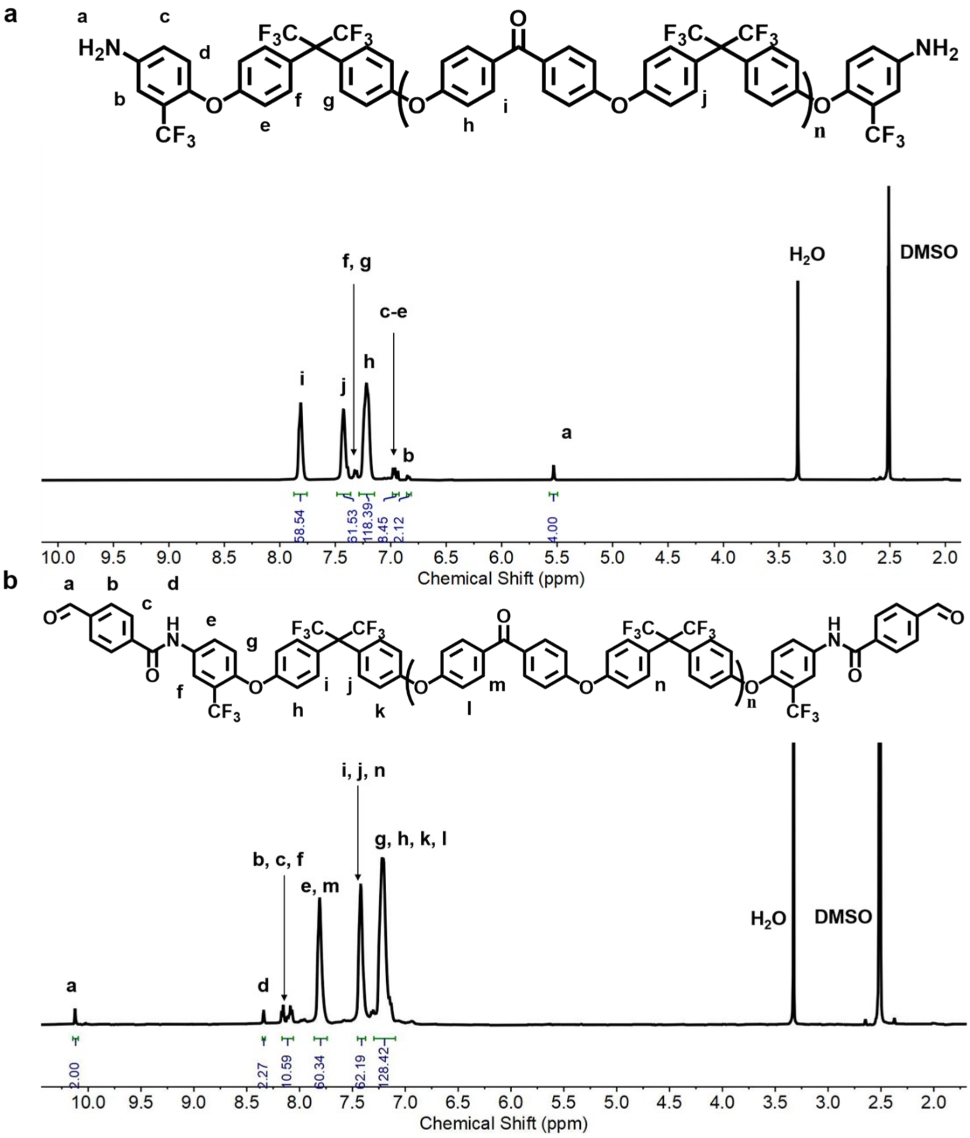

Fig. S8. ^{1}H NMR spectra of $PAEK_{8.2k}$ (a) and $PA_2EK_{8.2k}$ (b). According to the NMR data, the M_n of $PAEK_{8.2k}$ is ~8177.97.

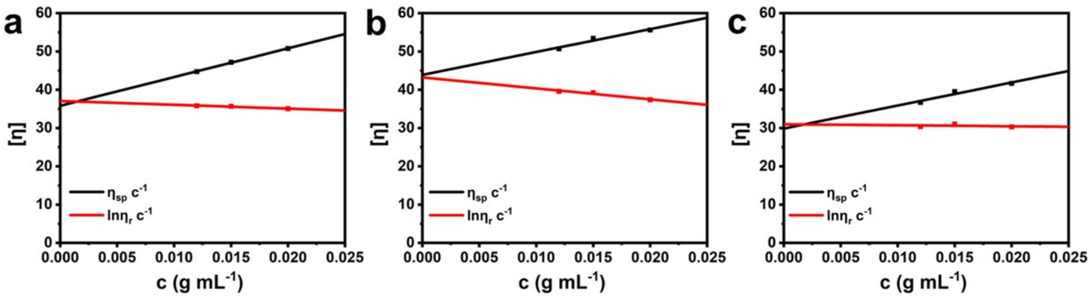

Fig. S9. Huggins-Kramer double plots for I-$PAEK_{2.6k}$ (a), I-PAEK (b) and I-$PAEK_{8.2k}$ (c) at 25 °C.

The intrinsic viscosities ([η]) of I-PAEK, I-$PAEK_{2.6k}$ and I-$PAEK_{8.2k}$ were determined using an Ubbelohde viscometer in NMP at 25 °C. The measurements were performed at different polymer concentrations (0.012, 0.015, and 0.020 g mL^{-1}), and the intrinsic viscosities were obtained from the y-intercepts of the Huggins and Kraemer plots.[1,2] The resulting intrinsic viscosities of I-PAEK, I-PAEK$_{2.6k}$, and I-PAEK$_{8.2k}$ are 43.55, 36.44, and 30.43 mL g^{-1}, respectively. According to the Mark-Houwink equation:

$$[\eta] = KM_v^{\alpha}$$

where K and α are Mark-Houwink constants, and M_v is the viscosity-average molecular weight. Therefore, a higher intrinsic viscosity generally indicates a higher viscosity-average molecular weight. Since I-PAEK has the highest viscosity, it is referred to possess the highest viscosity-average molecular weight.

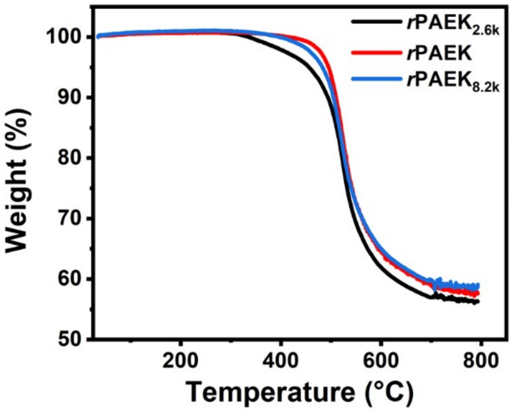

Fig. S10. TGA curves of *r*PAEK, *r*PAEK$_{2.6k}$ and *r*PAEK$_{8.2k}$ plastics.

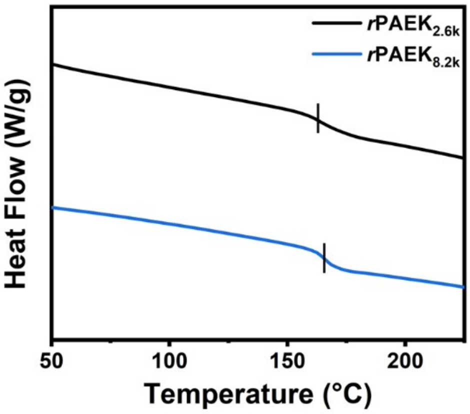

Fig. S11. DSC curves of the *r*PAEK$_{2.6k}$ and *r*PAEK$_{8.2k}$ plastics.

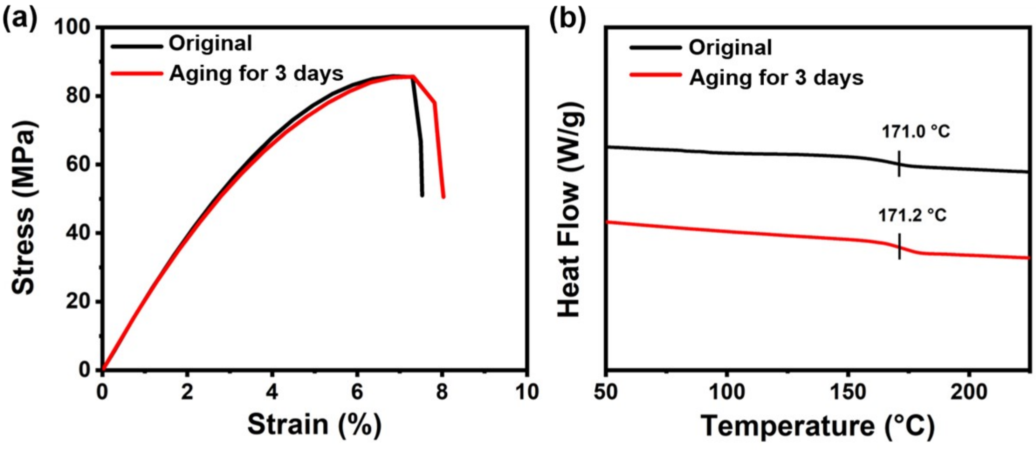

Fig. S12. Stress-strain (a) and DSC (b) curves of the original and aged *r*PAEK plastics after exposure to 70 °C and 100% relative humidity for 3 days.

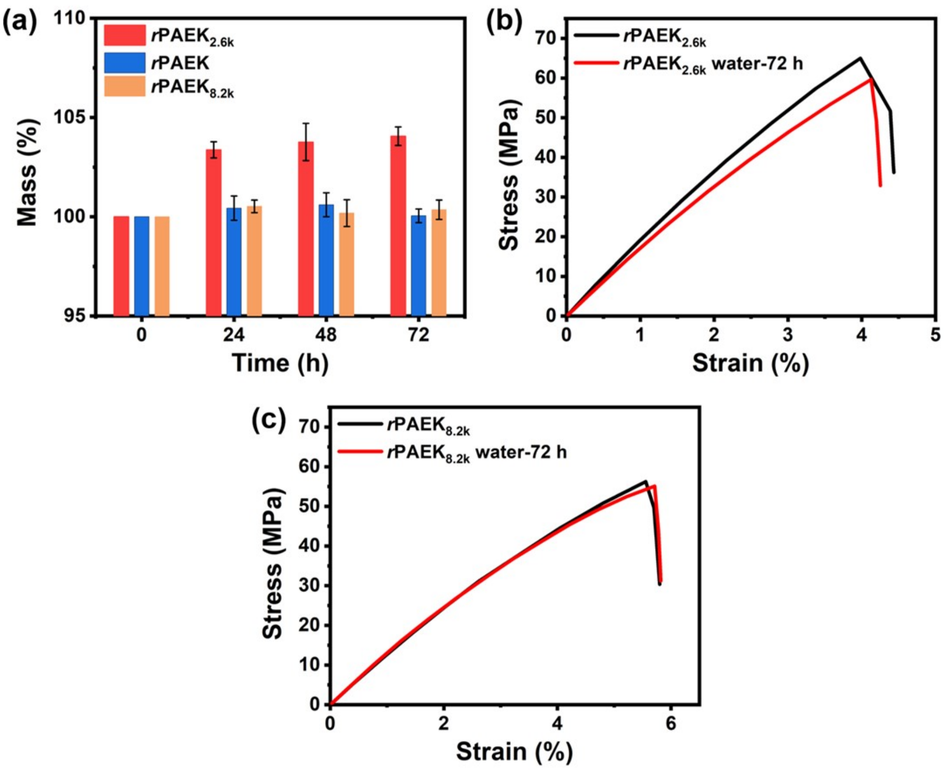

Fig. S13. (a) Relative mass changes of *r*PAEK$_{2.6k}$, *r*PAEK and *r*PAEK$_{8.2k}$ plastics after immersion in water for different durations. (b, c) Stress-strain curves of the pristine and water-soaked *r*PAEK$_{2.6k}$ plastics (b) and *r*PAEK$_{8.2k}$ (c) plastics.

As shown in Fig. S13a, *r*PAEK$_{2.6k}$ exhibits a relatively higher mass increase after immersion in water, with swelling ratios of ~103.4%, ~103.8%, and ~104.1% after soaking for 24, 48, and 72 h, respectively. In contrast, *r*PAEK$_{8.2k}$ shows only slight swelling over 72 h (~100.3%), comparable to that of *r*PAEK. Tensile tests were subsequently performed on the 72 h-soaked samples without drying. As shown in Fig. S13b, the soaked *r*PAEK$_{2.6k}$ plastics show an obvious decrease in mechanical performance, with the tensile strength decreasing from ~65.0 MPa to ~59.6 MPa and Young's modulus decreasing from ~2.00 GPa to ~1.75 GPa. In contrast, the mechanical performance of *r*PAEK$_{8.2k}$ remains almost unchanged after water immersion (Fig. S13c). This difference in water resistance originates from the different relative contents of imine linkages and amide groups in the *r*PAEK plastics. *r*PAEK$_{2.6k}$ contains a higher density of imine and amide groups per unit mass, which increases its affinity toward water and leads to a higher swelling ratio, accompanied by a reduction in mechanical performance after soaking. In contrast, *r*PAEK and *r*PAEK$_{8.2k}$ contain lower densities of these polar groups and higher fractions of hydrophobic aromatic PAEK segments, which effectively suppress water uptake and preserve the mechanical properties after immersion in water for 72 h.

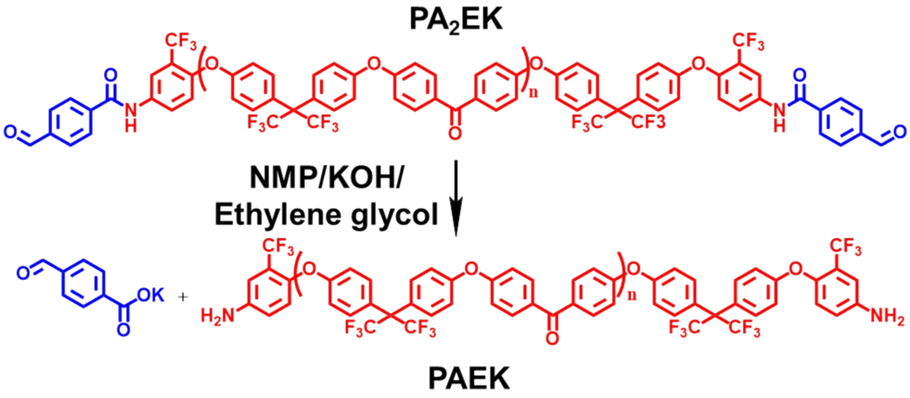

Fig. S14. Illustration of the alkaline hydrolysis of the amide groups in PA$_2$EK, leading to the formation of PAEK and potassium 4-formylbenzoate.

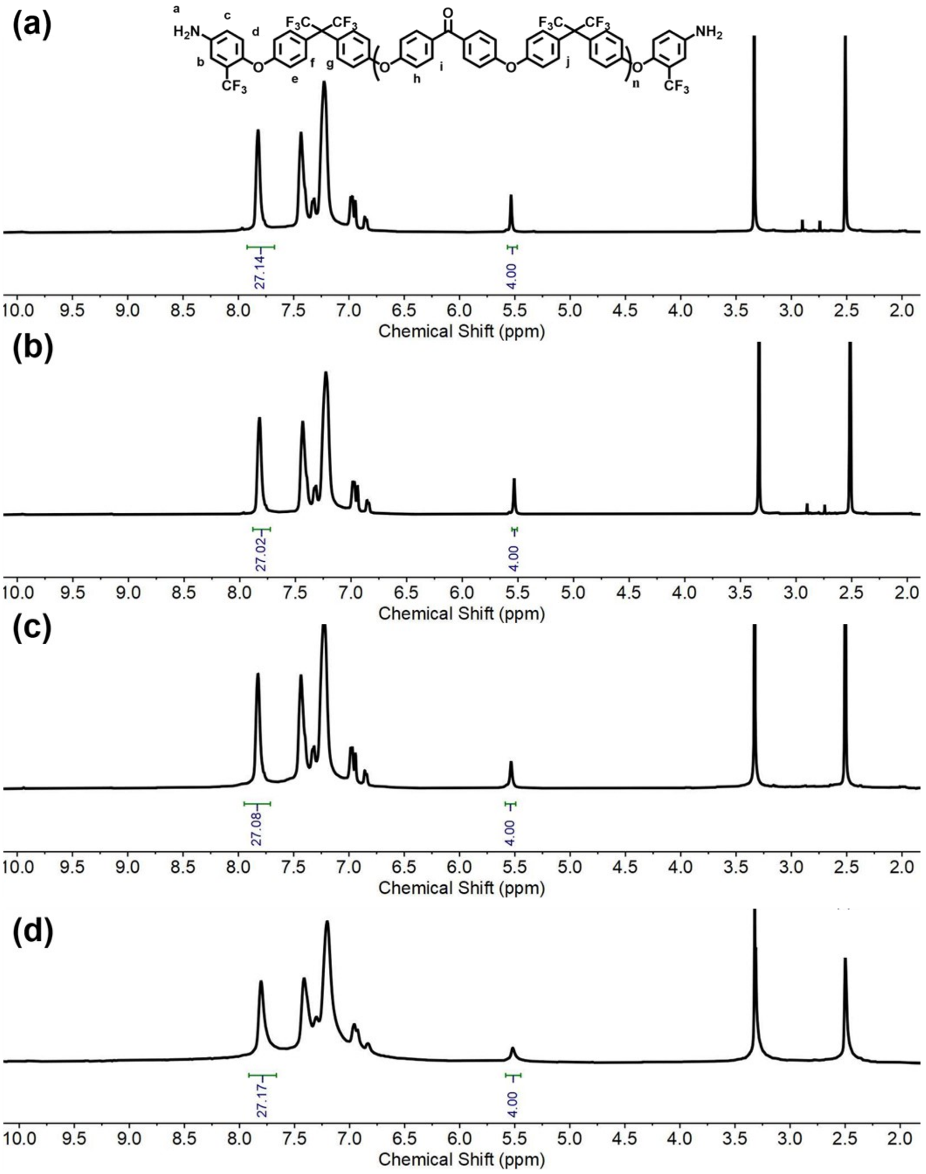

Fig. S15. ^{1}H NMR spectra of the original PAEK (a) and the recovered PAEK after the 1st (b), 2nd (c), and 3rd (d) recycling cycles. The integral ratio between peak i (aromatic protons adjacent to the carbonyl group) and peak a (terminal amino protons) remains nearly unchanged throughout the three recycling cycles. This result indicates that the molecular weight of the recovered PAEK is well maintained during the recycling process.

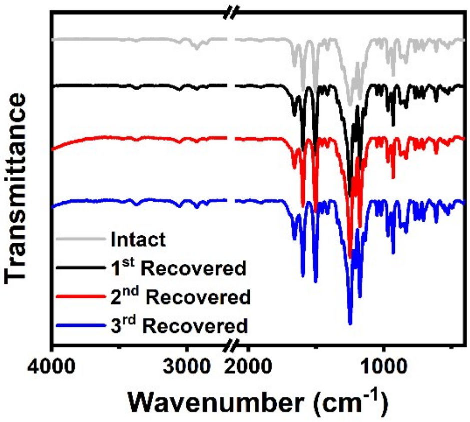

Fig. S16. FT-IR spectra of intact and recovered PAEK.

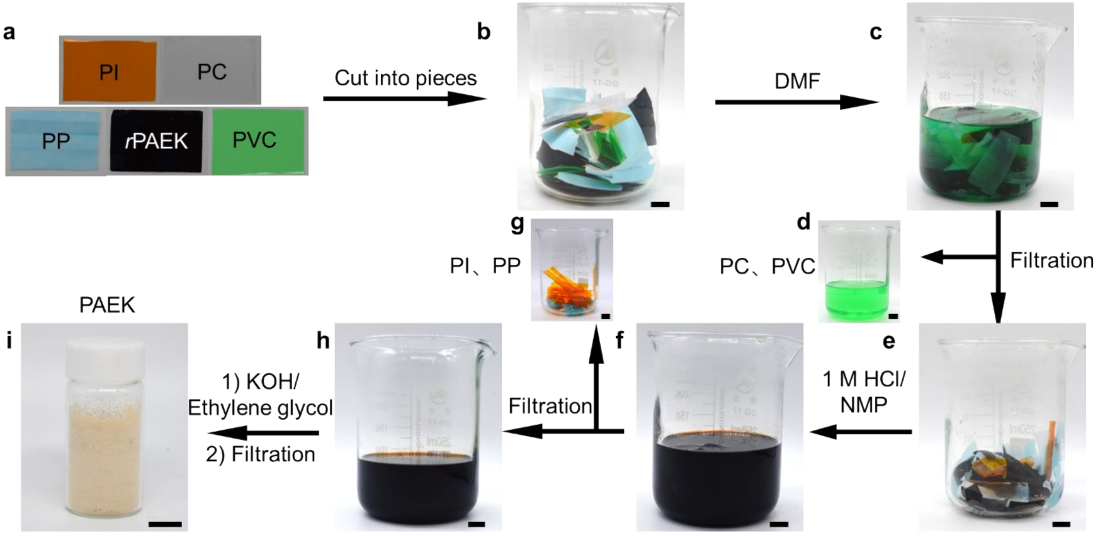

Fig. S17. Selective recycling of *r*PAEK plastics from mixed polymer wastes. Scale bars: 1 cm.

As shown in Fig. S17a, five types of plastic sheets were used, including yellow rubber tubes composed of polyimide (PI), colorless optical films composed of polycarbonate (PC), medical masks composed of polypropylene (PP), a green tablecloth composed of poly(vinyl chloride) (PVC), and *r*PAEK plastics. These plastics were cut into small pieces (Fig. S17b) and mixed to produce polymer waste (20 g). After adding DMF (100 mL), the PVC and PC pieces were dissolved (Fig. S17c) and subsequently removed by filtration (Fig. S17d). The remaining mixture containing *r*PAEK, PP, and PI (Fig. S17e) was treated with a mixed NMP/1 M HCl aqueous solution (105 mL, v/v = 6:1). After stirring for 4 h, the *r*PAEK plastics were dissolved and depolymerized into PAEK and PA$_2$EK, while the PP and PI pieces remained insoluble (Fig. S17f). The PP and PI pieces were removed by filtration (Fig. S17g), leaving a filtrate containing PAEK and PA_2EK (Fig. S17h). Using the same monomer conversion process in Fig. 3, PA_2EK was converted to PAEK (Fig. S17i).

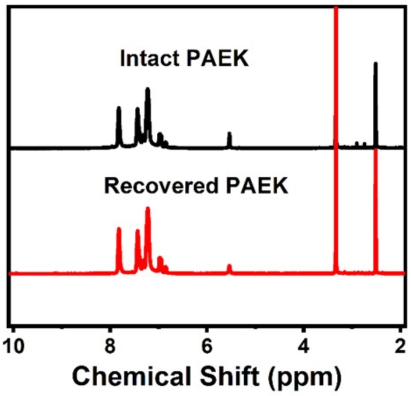

Fig. S18. ^1H NMR spectra for intact and recovered PAEK from the mixed plastic waste.

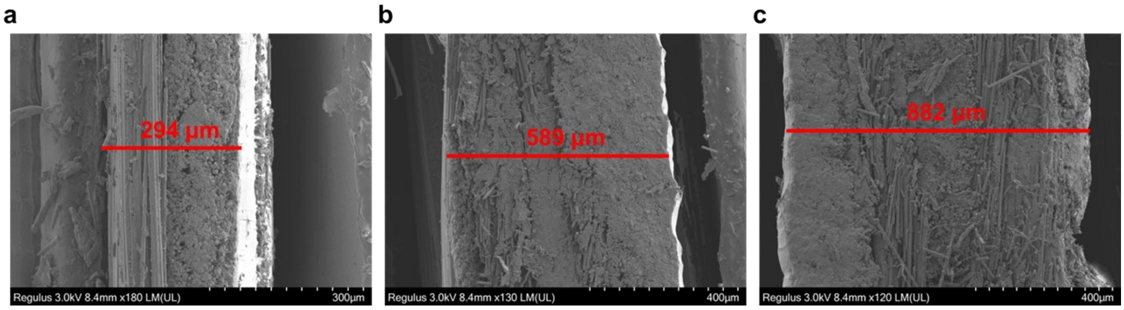

Fig. S19. Cross-section SEM images of 1- (a), 2- (b), and 3-CF-*r*PAEK composites (c).

Table S2. Summary of mechanical properties of n-CF-*r*PAEK plastics.

	Tensile Strength (MPa)	Young’s Modulus (GPa)	Flexural Strength (MPa)	Flexural Modulus (GPa)
1-CF-*r*PAEK	658 ± 21	16.1 ± 2.3	137 ± 7	14.3 ± 1.2
2-CF-*r*PAEK	675 ± 33	17.4 ± 2.1	362 ± 12	35.3 ± 2.7
3-CF-*r*PAEK	659 ± 26	18.9 ± 2.8	513 ± 19	39.1 ± 2.6

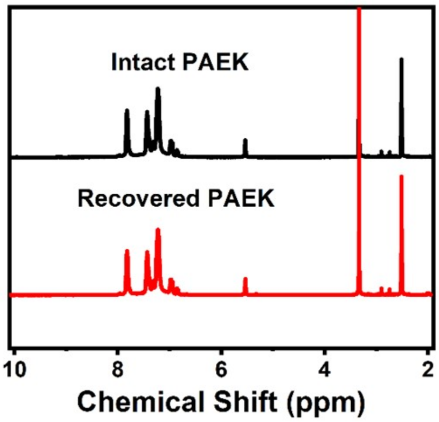

Fig. S20. ^{1}H NMR spectra for intact and recovered PAEK from 2-CF-*r*PAEK composites.

References

1 Fox, T. G., Jr.; Flory, P. J., Intrinsic Viscosity—Temperature Relationships for Polyisobutylene in Various Solvents1. *J. Am. Chem. Soc.* 1951**, 73** (5), 1909-1915.

2 Kim, I. C.; Tak, T. M., Synthesis of Soluble Anion-Exchange Copolyimides and Nanofiltration Membrane Performances. *Macromolecules* 2000**, 33** (7), 2391-2396.